Chemical Energy Release and Radical Formation in Cluster-Induced Sputtering of Diatomic Molecular Targets: A Molecular-Dynamics Model Study

Christian Anders and Herbert M. Urbassek*

Fachbereich Physik, Universität Kaiserslautern, Erwin-Schrödinger-Straße, D-67663 Kaiserslautern, Germany

(Received 3 January 2007; published 13 July 2007)

Using molecular-dynamics simulation, we perform a systematic study of cluster-induced sputtering. Two model systems of diatomic molecular solids are employed, which have identical cohesive energy but differ in their dissociation energy and the possible reaction pathways. Sputtering occurs by the flow of gasified material out of the spike volume into the vacuum above it. Because of the entrainment of radicals and reaction products with the flow, only a minority of this debris is left behind in the target. The excitation of internal molecular degrees of freedom (rotation and vibration) slightly reduces the sputter yield in comparison to the sputtering of an atomic system, while the chemical energy release due to exothermic reactions of radicals formed enhances the yield in proportion to the chemical energy release.

DOI: 10.1103/PhysRevLett.99.027602 PACS numbers: 79.20.Ap, 61.80.Az, 61.80.Lj, 79.20.Rf

While the understanding of sputter phenomena in elemental atomic targets has reached a mature level, sputter phenomena in condensed molecular targets still pose many unanswered questions [1–4]. Consider a single ion impact on a diatomic molecular target. What portion of the impact energy is used to excite the internal molecular degrees of freedom (rotation and vibration) and what portion goes into center-of-mass translational energy? Can the population of excited states be characterized as a thermal equilibrium? How many dissociations occur under irradiation? What is the role of the chemical energy if exothermal reactions occur? Because of the increased complexity of molecular targets, experimental and theoretical studies of the sputtering of diatomic systems have been rare [5].

In a broader context, interest in the sputtering of molecular systems has been revitalized and extended to phenomena occurring under cluster impact by the secondary-ion mass spectroscopy (SIMS) community [6]. Here, it has been found that huge sputter yields containing a high fraction of unfragmented molecules can be obtained by cluster impact on molecular targets [7,8]. A vital question for the performance of depth analyses using this technique is the following: To what extent is the irradiated target contaminated with impact debris, i.e., molecular fragments or reaction products—or has this debris been swept out and sputtered away?

From the simulational point of view, a molecular-dynamics approach is well suited to model all nonelectronic effects associated with particle impact into molecular solids. However, due to the computational complexity, until a few years ago, these studies were rare and concentrated on low-energy atom impact into diatomic molecular solids like O_2 and N_2 [9,10]. More recently, inspired by the demands of the SIMS community, large-scale simulations of the irradiation of thin overlayer or even bulk targets of larger (organic) molecules and polymers were performed [11,12].

In the present paper, we use molecular-dynamics simulations to perform a systematic model study aimed at illuminating some of the above questions. By comparing two molecular solids with identical intermolecular bonding but differing in their dissociation energy and possible reaction pathways the role of molecule dissociation and exothermic chemical reactions can be assessed. By further comparing to the sputtering of an analogous van-der-Waals bonded atomic system we can evaluate the role of internal molecular excitations for sputtering.

We study three different targets, an atomic Ar target as a well-studied reference case [13,14], and two model molecular targets. These consist of diatomic molecules, which we shall denote by A_2 and AB. In the A_2 molecule, only dissociation and molecule reformation are possible; this system hence is used to demonstrate the influence of the excitation of the internal molecular degrees of freedom and dissociation on the sputter yield reduction. In the AB molecule, additionally radical reactions are possible. In order to demonstrate the influence of the chemical energy release on the sputtering most clearly, here the case of a highly exothermic reaction and a small reaction barrier have been chosen; actually, these features are characteristic for an explosive. We note that explosives have indeed been used as a matrix material in plasma desorption mass spectrometry of proteins [15]; the resulting increased molecular ion yield was attributed to the chemical energy released in the reaction of the explosive.

The projectile consists of a spherical cluster containing 100 particles of the same species as the target [16] with total impact energy E. The amorphous target contains between 37 400 and 229 000 atoms. Both target and cluster were relaxed before the simulation was begun. Our simulations run until the sputter yields have saturated; this happens after around 20–40 ps. For each bombarding energy, up to five impacts were simulated to gather statistics.

The Ar interaction potential is a pair potential of the Lennard-Jones form [17,18], splined to the KrC potential

[19] valid for close Ar-Ar encounters. A_2 and AB molecules are modeled by the reactive empirical bond order approach developed by Brenner *et al.* [20,21] for the atomistic study of chemically sustained shock (detonation) waves; this modeling was inspired by the $2NO \rightarrow N_2 + O_2$ reaction. At close collisions the interaction potential is splined to the ZBL potential [22]. The A_2 molecule has a dissociation energy of $D_{AA} = 5$ eV, while the AB molecule is more weakly bound by $D_{AB} = 2$ eV. The B_2 interaction potential has identical properties as for the A_2 molecule. Hence the net reaction

$$2AB \rightarrow A_2 + B_2 \tag{1}$$

is exothermic with a reaction enthalpy $\Delta H_{\text{reac}} = 3$ eV per AB molecule. The reaction barrier of 0.08 eV is tiny. Further properties of the reactive potential are found in Refs. [20,21]. The intermolecular bonding is modeled by a Lennard-Jones potential, which is identical for the three molecules A_2, B_2, AB, and gives the crystalline solid a cohesive energy of $U = 107$ meV.

Figure 1 displays the dependence of the sputter yield Y as a function of the scaled impact energy E/U. Linear fits of the form [13]

$$Y = \alpha(E - E_{\text{th}})/U \tag{2}$$

describe the data quite well. Here E_{th} is a sputter threshold and α denotes the sputter efficiency. Our fit gives $\alpha = 0.054\ (0.084, 0.133)$ and $E_{\text{th}}/U = 200\ (2010, 2750)$ for the A_2 (Ar, AB) target. Note furthermore that the sputter efficiency α for the Ar target is slightly larger than that reported in Ref. [13], since in the present simulation we took care to employ a sufficiently large target and a long simulation time to obtain saturated sputter yields.

From scaling considerations [13,23], it is known that the yields for all (atomic) Lennard-Jones materials should be identical if scaled energy units E/U are used. Evidently, for not too small impact energies, $E/U \gtrsim 8000$, the A_2 yields are smaller than the Ar yields. This can be quantified by a ratio of the sputter efficiencies $\alpha_{AA}/\alpha_{\text{Ar}} = 0.64$. We suggest that the reason hereto lies in the internal excitation of molecules in the irradiated A_2 sample and prove it as follows: Fig. 2 displays the partitioning of the kinetic energy of free molecules sputtered from the sample. It shows that 10%–20% of the kinetic-energy content of sputtered molecules is internal energy. This partitioning demonstrates that only 80%–90% of the impact energy has been used for sputtering, while the rest is used for internal heating of the molecules. This quantitatively explains the ratio of $\alpha_{\text{Ar}}/\alpha_{AA}$ reported above.

The AB target behaves analogously to A_2 up to an energy of around $E/U = 5000$. Above this threshold the AB yield strongly increases in a nonlinear way above the yields of the other targets. Figure 2(b) demonstrates that at the same energy vibrational excitation is strongly enhanced. This is due to the fact that at this impact energy AB dissociation becomes possible, and hence the exothermic reaction (1) starts, which creates vibrationally hot product molecules. Note that at the scaled energy $E/U = 5000$, each of the 100 projectile molecules has a kinetic impact energy of 5 eV and thus has kinematically the possibility to impart the dissociation energy $D_{AB} = 2$ eV as internal energy to a target molecule in a central collision. Because of the high reaction exothermicity, it might be surmised that projectile impact into the AB target may initiate a detonation wave in the material [20]. We did not find any indication of this and presume that this is due to the fact that the "detonation front" spreads out hemispherically in three dimensions, and hence its energy density sinks rapidly during propagation.

As an aside we note that the distribution of the energy onto the various degrees of freedom shown in Fig. 2 is far from thermal equilibrium. In statistical equilibrium rotation would receive double as much kinetic energy as vibration. For the A_2 molecule this is—at least for $E/U < 20\,000$—not the case, since vibrational excitation

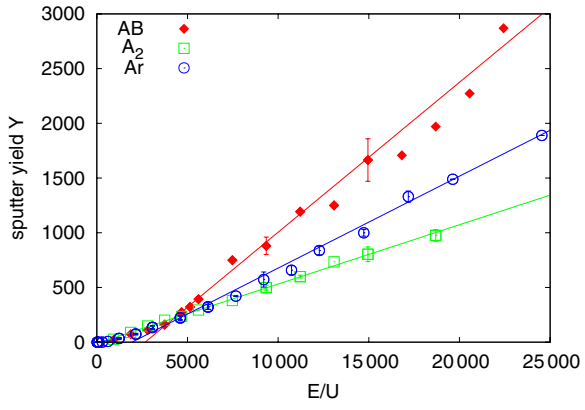

FIG. 1 (color online). Sputter yield Y vs scaled bombarding energy E/U. The yield is measured in units of atoms for the Ar solid and in molecules otherwise. The lines are linear fits, Eq. (2).

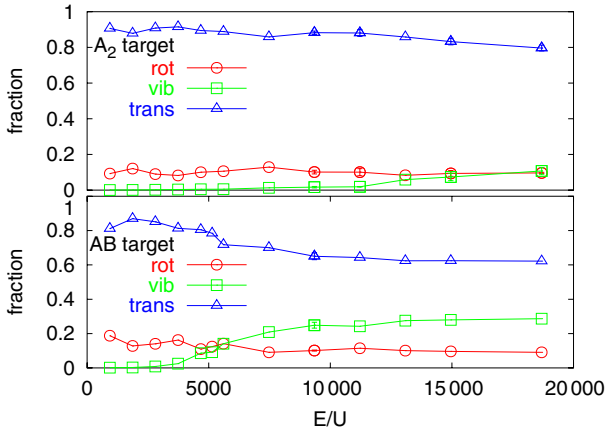

FIG. 2 (color online). Distribution of kinetic energy of free molecules sputtered from an A_2 target (top) and an AB target (bottom) into translational, rotational, and vibrational degrees of freedom.

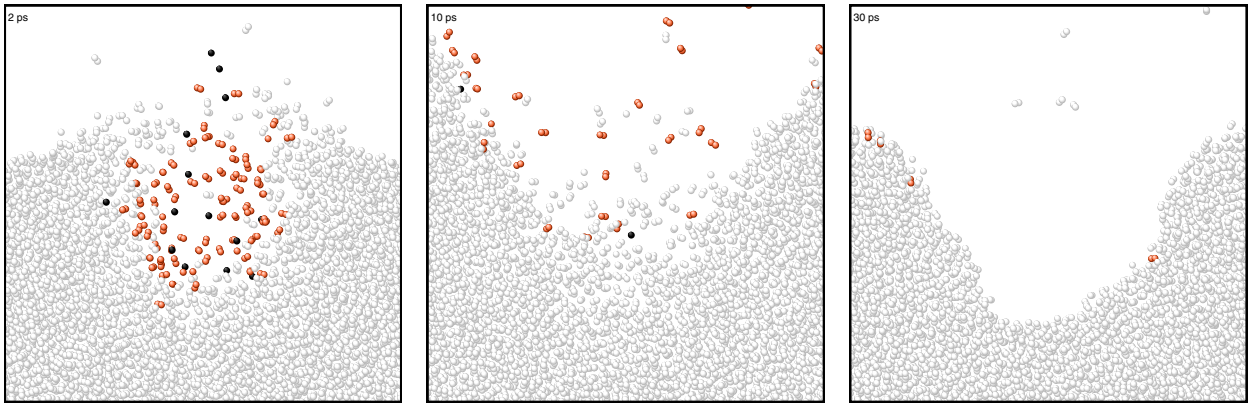

FIG. 3 (color online). Cross-sectional view (thickness 10 Å) through the irradiated AB target at several times after impact at $E/U = 10\,000$. Only the central part (113 Å wide) is shown. Light gray: original AB molecules. Dark gray (red): reaction products, A_2 and B_2. Black: radicals (atoms).

is quenched due to a vibrational adiabaticity argument [24]. In the AB target, on the other hand, reaction products are vibrationally hot, and thus thermal equilibrium is not reached in the expanding sputter flow.

Figure 3 shows an atomistic representation of the impact and sputter process in the AB target at 3 times after impact. In the spike region, almost no native AB molecules have survived. They have been dissociated and most of the radicals formed have already reacted. Note that due to the high vibrational excitation of the product molecules, it is likely that they convey energy to their neighbors; this helps them in ''evaporating'' off the surface. At the end of the sputter process, at $t = 30$ ps, only a few product molecules, which are embedded in the wall of the resulting crater, have remained in the target.

Figure 4(a) displays the partial sputter yields of the AB target and demonstrates that at the threshold energy of $E/U \cong 5000$ radical and product emission starts. The number of radicals sputtered is very small as most of them have reacted to A_2 and B_2 molecules. Figure 4(b) presents the fraction of radicals and product molecules which remain in the target. It shows an interesting energy dependence. While close to the production threshold at $E/U \cong 5000$ the majority remains in the target, at higher bombarding energies the fraction decreases to below 30%. We can hence conclude that the sputter process itself is very efficient in cleaning the target of radicals and products.

Let us finally discuss the role of dissociations and reactions on the energetics of sputtering. Figure 5 displays the number N_{ex} of bond changes occurring, i.e., the number of molecules, in which two new partners are bound. Again, the results are well described by linear fits of the form (2) with $\alpha = 0.054\,(0.015)$ and $E_{\mathrm{th}}/U = 3700\,(10\,000)$ for the AB (A_2) target. In agreement with the higher dissociation energy of A_2 molecules, the threshold in the A_2 target is a factor of roughly $D_{AA}/D_{AB} = 2.5$ higher.

If all the impact energy were used for dissociations, and all radicals reacted, a maximum number of $(N_{\mathrm{ex}})_{AA} = E/D_{AA} = 0.021E/U$ of bond breaks (and exchanges) could be expected in the A_2 target. A more detailed calculation [5], including collision-cascade statistics and the fact that in a two-molecule collision only part of the impact energy can be used for bond breaking, adds a factor of $\frac{1}{4}$. This estimate semiquantitatively explains the linear increase of the A_2 bond breaks with impact energy. We

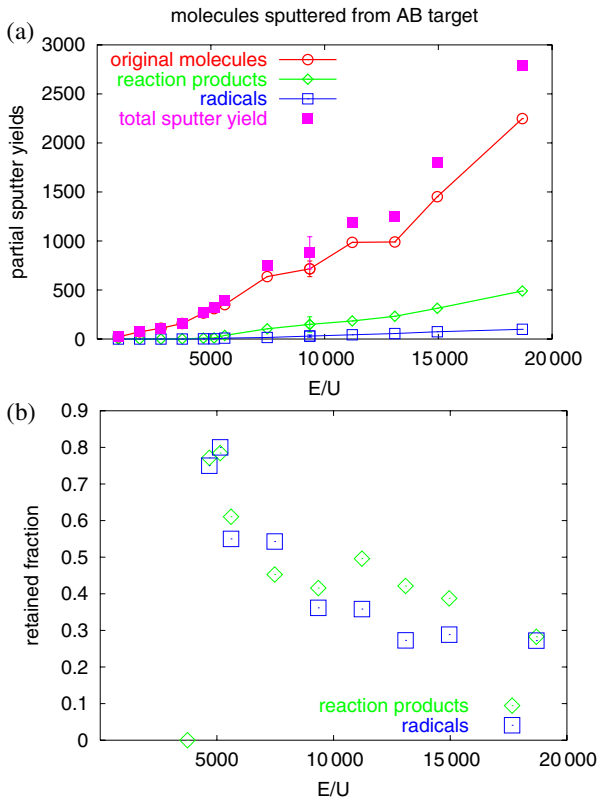

FIG. 4 (color online). Production of radicals and reaction products induced by impact on an AB target with scaled energy E/U. (a) Partial sputter yields. (b) Fraction of reaction products and radicals retained in the target.

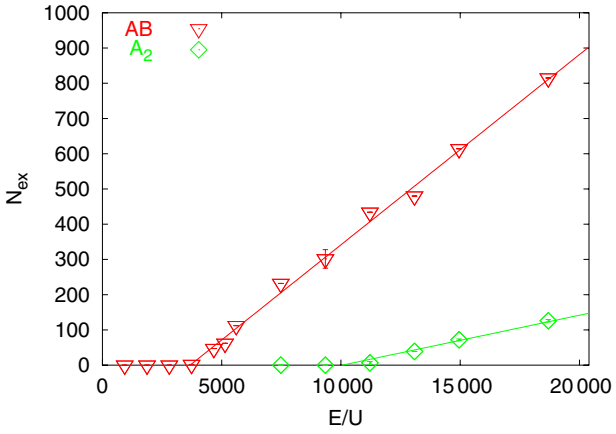

FIG. 5 (color online). Number of bond changes N_{ex} in the AB and the A_2 target after impact with scaled energy E/U.

note that at the end of the simulation, the number of dissociated A_2 molecules amounts to only 8% of N_{ex}. In the AB system, a similar estimate results in $(N_{ex})_{AB} = E/D_{AB} = 0.05E/U$.

The number of reactions occurring in the AB target (measured as the number of reaction products formed) amounts to $N_{reac} = 0.045(E/U - 3700)$ (not shown). This allows us to estimate the chemical energy release due to the exothermic reactions as

$$\Delta E_{chem} = N_{reac}\Delta H_{reac} = 0.045(\Delta H_{reac}/U)E = 1.3E, \quad E \gg 5000U, \tag{3}$$

where the constant term describing the threshold has been neglected. Since ΔE_{chem} is linear in the impact energy [5] an inclusion of the chemical energy would thus reproduce Eq. (2), but increase the sputter efficiency by 130%. This quantitatively explains the strong increase in the sputter efficiency of the AB target ($\alpha_{AB} = 0.133$) with respect to the A_2 target ($\alpha_{AA} = 0.054$). Equation (3) is a central result, since it demonstrates how to quantify the effect of the chemical energy release on sputtering.

In conclusion, we have employed two model systems of diatomic molecular solids to perform a systematic molecular-dynamics study of cluster-induced sputtering. The sputter process occurs by the flow of gasified material out of the spike volume into the vacuum above it. Because of the entrainment of radicals and reaction products with the flow, only a minority of this debris is left behind in the target. Almost all radicals react in the highly excited spike volume. We showed that the excitation of the internal molecular degrees of freedom (rotation and vibration) slightly reduces the sputter yield in comparison to the sputtering of an atomic system. The chemical energy release due to exothermic reactions of radicals formed enhances the yield in proportion to the chemical energy release. Sputtered molecules are not in thermal equilibrium with each other: Their internal energy amounts to only 10%–20% of the translational energy.

*urbassek@rhrk.uni-kl.de; http://www.physik.uni-kl.de/urbassek/

[1] *Sputtering by Particle Bombardment I*, edited by R. Behrisch (Springer, Berlin, 1981).
[2] Special issue on Fundamental Processes in Sputtering of Atoms and Molecules, edited by P. Sigmund [K. Dan. Vidensk. Selsk. Mat. Fys. Medd. **43** (1993)].
[3] R. A. Baragiola, Phil. Trans. R. Soc. A **362**, 29 (2004).
[4] Special issue on Ion Beam Science: Solved and Unsolved Problems, edited by P. Sigmund [K. Dan. Vidensk. Selsk. Mat. Fys. Medd. **52** (2006)].
[5] V. Balaji, D. E. David, R. Tian, J. Michl, and H. M. Urbassek, J. Phys. Chem. **99**, 15 565 (1995).
[6] N. Winograd, Anal. Chem. **77**, 142A (2005).
[7] D. Weibel, S. Wong, N. Lockyer, P. Blenkinsopp, R. Hill, and J. C. Vickerman, Anal. Chem. **75**, 1754 (2003).
[8] I. Bolotin, S. Tetzler, and L. Hanley, Appl. Surf. Sci. **252**, 6533 (2006).
[9] H. Kafemann and H. M. Urbassek, Mod. Phys. Lett. B **7**, 857 (1993).
[10] L. Dutkiewicz, R. E. Johnson, A. Vertes, and R. Pedrys, J. Phys. Chem. A **103**, 2925 (1999).
[11] A. Delcorte, P. Bertrand, and B. J. Garrison, J. Phys. Chem. B **105**, 9474 (2001).
[12] B. Czerwinski, A. Delcorte, B. J. Garrison, R. Samson, N. Winograd, and Z. Postawa, Appl. Surf. Sci. **252**, 6419 (2006).
[13] C. Anders, H. M. Urbassek, and R. E. Johnson, Phys. Rev. B **70**, 155404 (2004).
[14] C. Anders and H. M. Urbassek, Nucl. Instrum. Methods Phys. Res., Sect. B **228**, 84 (2005).
[15] K. Hakansson, R. A. Zubarev, R. V. Coorey, V. L. Talrose, and P. Hakansson, Rapid Commun. Mass Spectrom. **13**, 1169 (1999).
[16] 100 Ar atoms in the case of the Ar target and 100 molecules in the case of the molecular target.
[17] A. Michels, H. Wijker, and H. K. Wijker, Physica (Amsterdam) **15**, 627 (1949).
[18] J.-P. Hansen and L. Verlet, Phys. Rev. **184**, 151 (1969).
[19] W. D. Wilson, L. G. Haggmark, and J. P. Biersack, Phys. Rev. B **15**, 2458 (1977).
[20] D. W. Brenner, D. H. Robertson, M. L. Elert, and C. T. White, Phys. Rev. Lett. **70**, 2174 (1993).
[21] D. W. Brenner, MRS Bull. **21**, 36 (1996).
[22] J. F. Ziegler, J. P. Biersack, and U. Littmark, *The Stopping and Range of Ions in Solids* (Pergamon, New York, 1985).
[23] H. M. Urbassek, H. Kafemann, and R. E. Johnson, Phys. Rev. B **49**, 786 (1994).
[24] R. D. Levine and R. B. Bernstein, *Molecular Reaction Dynamics and Chemical Reactivity* (Oxford University Press, Oxford, 1987).